THE GEOLOGICAL SOCIETY OF AMERICA®

High-angle, not low-angle, normal faults dominate early rift extension in the Corinth Rift, central Greece

Rebecca E. Bell[1], Guillaume Duclaux[2]*, Casey W. Nixon[2], Robert L. Gawthorpe[2], and Lisa C. McNeill[3]
[1]Basins Research Group, Imperial College London, Prince Consort Road, South Kensington, London SW7 2BP, UK
[2]Department of Earth Science, University of Bergen, P.O. Box 7803, N-5020 Bergen, Norway
[3]Ocean and Earth Science, National Oceanography Centre Southampton, University of Southampton, European Way, Southampton SO14 3ZH, UK

ABSTRACT

Low-angle normal faults (LANFs) accommodate extension during late-stage rifting and breakup, but what is more difficult to explain is the existence of LANFs in less-stretched continental rifts. A critical example is the <5 Ma Corinth Rift, central Greece, where microseismicity, the geometry of exposed fault planes, and deep seismically imaged faults have been used to argue for the presence of <30°-dipping normal faults. However, new and reinterpreted data call into question whether LANFs have been influential in controlling the observed rift geometry, which involves (1) exposed steep fault planes, (2) significant uplift of the southern rift margin, (3) time-averaged (tens of thousands to hundreds of thousands of years) uplift-to-subsidence ratios across south coast faults of 1:1–1:2, and (4) north margin subsidence. We test whether slip on a mature LANF can reproduce the long-term (tens of thousands of years) geometry and morphology of the Corinth Rift using a finite-element method, to model the uplift and subsidence fields associated with proposed fault geometries. Models involving LANFs at depth produce very minor coseismic uplift of the south margin, and post-seismic relaxation results in net subsidence. In contrast, models involving steep planar faults to the brittle-ductile transition produce displacement fields involving an uplifted south margin with uplift-to-subsidence ratios of ~1:2–3, compatible with geological observations. We therefore propose that LANFs cannot have controlled the geometry of the Corinth Rift over time scales of tens of thousands of years. We suggest that although LANFs may become important in the transition to breakup, in areas that have undergone mild stretching, do not have significant magmatic activity, and do not have optimally oriented preexisting low-angle structures, high-angle faulting would be the dominant strain accommodation mechanism in the upper crust during early rifting.

INTRODUCTION

Both high- and low-angle (dipping <30°) normal faults have been proposed to accommodate strain at some early-stage continental rifts, including the Basin and Range (North America), central Apennines (Italy), Aegean–western Turkey, and Corinth Rift (Greece). Low-angle normal faults (LANFs) present a paradox in structural geology, as Andersonian theory (Anderson, 1905) would suggest that slip on LANFs is mechanically unfavorable. These continental rifts are therefore crucial case studies for assessing when in the rifting process, and under what conditions, LANFs become important in accommodating strain. In the Basin and Range, an association between detachments (faults dipping <15°) and magmatic activity has been reported, suggesting that igneous midcrustal inflation may rotate the stress field such that LANFs are favorable (Parsons and Thompson, 1993). Low-angle faults have been observed in Turkey, however these may have rotated from steeper angles to their current 0°–20° dip angles (Gessner et al., 2001), rather than LANFs being a first-order extension mechanism. Low-angle normal faults have also been observed in the central Apennines, where their origin has been linked to subduction rollback (Collettini et al., 2006) or collapse of an overthickened accretionary wedge, whereby thrust faults are reactivated as LANFs (Ghisetti and Vezzani, 1999). These studies suggest that LANFs are only present in early-stage continental rifts under rather specific conditions.

A key example is the 3–30-km-wide Corinth Rift, Greece, which at <5 Ma and with a stretching factor (initial crustal thickness divided by final crustal thickness) of <1.4 (Bell et al., 2011), provides a snapshot of the very early stages of continental rifting (Fig. 1A). The western part of the rift has

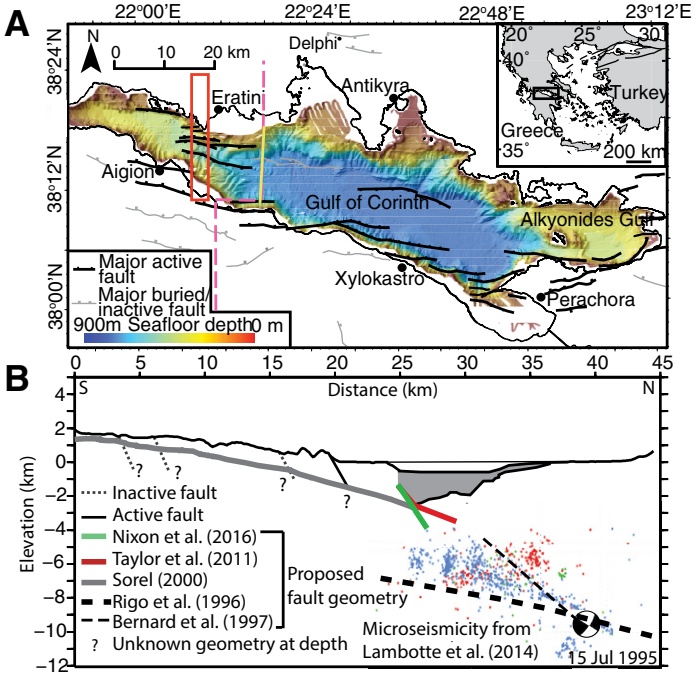

Figure 1. A: Corinth Rift (central Greece) bathymetry and major active and inactive faults. Red box shows location of microseismicity data in B. Yellow line shows location of seismic profile in Fig. DR1 (see footnote 1). Pink dashed line shows location of profile in B. B: Composite cross section across western Corinth Rift to show proposed deep fault geometry models. Dark gray represents syn-rift fill offshore; onshore syn-rift fill is not represented. Microseismicity is from Lambotte et al. (2014): blue dots are micoseismicity between A.D. 2000 and 2007; red dots, 1995; green dots, 1991. Note that microseismicity data have been projected onto this profile from further west. Focal mechanism is for 15 July 1995 earthquake (Bernard et al., 1997).

*Current address: Université Côte d'Azur, CNRS, OCA, IRD, Géoazur, 06560 Valbonne, France.

long been used as an example of a setting where low-angle normal faulting plays a key role in strain accommodation (e.g., Jolivet et al., 2010; Sorel, 2000) and is commonly referred to by studies reviewing LANF mechanisms (e.g., Lecomte et al., 2012). The Corinth Rift is amagmatic, and like the central Apennines, it occurs within orogenically thickened crust; however, the Corinth Rift runs orthogonal, not parallel, to the Hellenide orogeny. If early-stage continental extension at the Corinth Rift is really controlled by LANFs, it would suggest that they may be a primary strain-accommodation mechanism in the earliest stages of continental rifting.

If a mature, seismically active LANF or detachment does exist beneath the western Corinth Rift, slip on such a structure must be able to account for the long-term (tens of thousands to hundreds of thousands of years) geometry and pattern of vertical displacement across the rift, which is well constrained from seismic reflection imaging and geomorphology data. The southern margin is uplifting with late Quaternary uplift rates of 0.8–2.0 mm/yr determined from uplifted marine terraces and wave-cut notches (e.g., Armijo et al., 1996). Long-term uplift-to-subsidence ratios across the largest faults bordering the southern margin are estimated at 1:1.2 – 1:2.2, measured from the elevation of features of comparable age in the footwall and hanging wall (McNeill et al., 2005, 2007). In contrast, the northern margin appears to be dominated by subsidence (Bell et al., 2009; Elias et al., 2009). GPS data have been collected in the Corinth Rift; however, Bell et al. (2011) showed that GPS extension rate patterns are incompatible with the long-term rift geometry and cannot have persisted over a 100+ k.y. time scale.

In this study, we perform new finite-element displacement modeling to investigate if LANFs are capable of reproducing the observed patterns of vertical displacement across the rift to definitively address the question: Is Corinth an example of a rift that is dominated by low-angle normal faulting? If the answer to this question is no, the elimination of this example would call into question the significance of LANFs during early-stage rifting.

LOW-ANGLE VERSUS HIGH-ANGLE DEEP FAULT GEOMETRY MODELS IN THE CORINTH RIFT

The shallow geometry of Corinth Rift active faults is known from exposed fault scarps onshore, with reported fault dips of 46°–60° (e.g., Ford et al., 2013). Seismic reflection interpretations from different authors agree that the dip angle of offshore faults down to ~3 km ranges from 35° to 60° (e.g., Nixon et al., 2016; Taylor et al., 2011). However, controversy remains as to the geometry of faults deeper than 3 km as these have never been directly imaged. Two classes of deep fault geometry model have emerged.

Low-Angle (<30°) Active Faults at Depths >3 km

Rigo et al. (1996) proposed that microseismicity lies on a plane dipping 10°–25° to the north at a depth of ~6–9 km below the south coast of the Gulf of Corinth (Fig. 1B). They interpreted this band of active seismicity as a low-angle detachment onto which steep faults observed at the surface sole at depth. Syn-rift sediment depocenters in the northwestern Peloponnese have shifted north through time, and although most of the faults in this area are moderately to steeply dipping (40°–50°), the most southern and oldest fault is low-angle (25°). Sorel (2000) proposed that this structure is a detachment extending northwards beneath observed steep faults in the western part of the rift (Fig. 1B). Sachpazi et al. (2003) and Taylor et al. (2011) interpreted from deep seismic reflection data a low-angle structure at a similar depth to Sorel's (2000) proposed detachment in the western rift (Fig. 1B; Fig. DR1 in the GSA Data Repository[1]). Some focal mechanisms determined for large (M 6) earthquakes that have occurred in the western rift may support relatively low-angle faulting, however these are subject to the nodal plane that is selected as the active fault (Bernard et al. 1997).

Although Rigo et al. (1996) and Sorel (2000) are commonly cited together as studies in support of a low-angle detachment, the Sorel (2000) and Taylor et al. (2011) LANF is 3 km beneath the south coast of the gulf, whereas the zone of microsesimicity is at 6–9 km depth (Fig. 1B).

Moderate-Angle to High-Angle Faults (35°–60°) to Depths >3 km

Although there is debate regarding the western Corinth Rift, focal mechanisms of large earthquakes in the eastern rift occurred on faults dipping at 40°–50° (Jackson et al., 1982). Lambotte et al. (2014) resolved the western Corinth Rift seismicity pattern further, and noted that, in some locations, the microseismicity cloud appears to dip 10°–20° to the north, yet in others, it is subhorizontal or chaotic (Fig. 1B). They also observed seismicity beneath the clustered microseismicity cloud, which they suggested is the continuation of high-angle faults imaged at shallower depth and supports a high-angle fault model rather than an active detachment. Nixon et al. (2016) reinterpreted the deep seismic reflection data and suggested that north-dipping south margin faults remain moderately to steeply dipping (35°–60°) below depths of 3 km (Fig. 1B; Fig. DR1). Further evidence for high-angle faulting comes from McNeill et al. (2005), Bell et al. (2011), and Ford et al. (2013), who calculated total extension across the rift by summing fault heaves assuming a planar fault geometry. In the western Corinth Rift, the amount of extension required for the observed basement subsidence and crustal thinning is in line with summed heaves across higher-angle faults.

MODELING THE VERTICAL DISPLACEMENT FIELD

We use PyLith (https://geodynamics.org/cig/software/pylith/), a finite-element code with quasi-static formulation (Aagaard et al., 2013), to model the deformation associated with imposed fault slip in a simple layered continental crust, and we solve the two-dimensional (2-D) surface uplift and subsidence fields for the two contrasting fault geometry models. PyLith allows the coseismic displacement field associated with a particular magnitude of slip on a fault to be calculated and also the deformation associated with post-seismic relaxation to be recovered. Assuming linear rheologies, addition of these displacement fields is representative of the vertical deformation pattern caused by multiple seismic cycles over a 10+ k.y. time scale.

Our 2-D model includes a 10-km-thick elastic upper crust overlying a 30-km-thick viscoelastic lower crust layer with a Newtonian rheology with constant viscosity of 10^{19} Pa·s, consistent with previously published models for the region (Fig. 2; Sachpazi et al., 2007; King, 1998). The Maxwell time for the viscoelastic material is 10 yr, and full relaxation of the model is achieved after ~30 k.y. (Fig. DR2). The model is 1000 km wide, with free-slip boundary conditions on the model sides and base and a top free surface. We only consider deformation patterns in the central 100 km of the model to avoid boundary effects. We impose a total of 200 m of normal slip along a prescribed fault (simulating the result of 30 k.y. of earthquakes with a recurrence interval of 150 yr and a displacement of 1 m) and let the system relax. We present our vertical deformation results normalized to show the amount of uplift and subsidence produced per meter of displacement on the fault and compare them to first-order

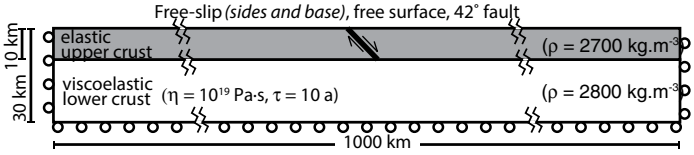

Figure 2. Finite-element model setup. Open circles indicate free-slip boundaries. ρ is density, τ is Maxwell time, and η is viscosity.

[1]GSA Data Repository item 2018025, Figures DR1 (high- and low-angle faults interpreted in seismic data), DR2 (variation in vertical displacement with postseismic relaxation), DR3 (horizontal displacement for low- and high-angle faults), and DR4–DR6 (the effect of changing model layer thickness), is available online at http://www.geosociety.org/datarepository/2018/ or on request from editing@geosociety.org.

observations of Corinth Rift vertical deformation. We also calculate the normalized horizontal deformation (extension produced per meter of fault displacement) between points 10 km on either side of the fault, to test how the magnitude of extension varies on high-angle versus low-angle faults (Fig. DR3). We note that varying elastic and viscous layer thickness within realistic limits does not change the conclusions presented in this manuscript (Figs. DR4–DR6). Changing the linear viscosity only changes the time scale of relaxation, not the final uplift-to-subsidence pattern.

To cover the full range of deep fault geometries proposed in the literature, we test two classes of fault model. Model 1 involves a LANF at depth, and two different scenarios are tested: (1) model 1a is a planar fault with dip of 45° that soles into a 15° north-dipping detachment at a depth of 7 km below the south coast (cf. Rigo et al., 1996); and (2) model 1b is a 45° fault that changes to a dip angle of 20° at a depth of 3 km and extends to a brittle-ductile transition at 10 km depth (cf. Sorel, 2000; Taylor et al., 2011). Model 2 involves planar faults that dip at 45° (model 2a) or 60° (model 2b) to the brittle-ductile transition at a depth of 10 km (after Nixon et al., 2016).

Model 1

The coseismic vertical displacement field associated with moderately high-angle faults (45°) soling into a detachment at a depth of 7 km (model 1a) and 3 km (model 1b) generates a minor amount of coseismic uplift of the southern margin (<0.01 m for every 1 m of slip), but an order of magnitude more uplift of the northern margin 20–25 km north of the surface trace of the fault (0.1 m for every 1 m of slip) (Figs. 3A and 3B). The coseismic uplift of the north margin occurs above where the low-angle fault tips out, as is also observed in dislocation models for low-angle normal faulting (e.g., Resor, 2008). The horizontal displacement between points 10 km either side of the fault associated with the coseismic response is 0.6–0.65 m of extension per meter of slip on the fault (Fig. DR3). After 30 k.y. of post-seismic relaxation, the overall vertical displacement profile changes considerably (Figs. 3A and 3B). The deformation across the rift associated with models 1a and 1b involves overall subsidence of both the southern and northern margins (Figs. 3A and 3B). This contrasts markedly with the observed uplift (0.8–2 mm/yr) of the southern Gulf of Corinth coastline averaged over a time scale of 10–100+ k.y.

Model 2

For both 45° and 60° normal faults (models 2a and 2b), the model predicts considerable coseismic uplift of the southern margin (0.12 m and 0.22 m for every 1 m of slip for 45° and 60° faults, respectively) and subsidence of the northern margin (Figs. 3C and 3D). The horizontal displacement between points 10 km either side of the fault associated with the coseismic response is 0.5 m of extension per meter of slip for model 2a, and 0.3 m of extension per meter of slip for model 2b (Fig. DR3). After post-seismic relaxation, the southern margin remains uplifted and the northern margin subsides.

DISCUSSION AND CONCLUSIONS

Deformation associated with LANFs modeled over a >10 k.y. time scale produces subsidence of the southern margin of the Corinth Rift, incompatible with the widespread indicators of uplift along the south coast (Figs. 3A and 3B). We suggest that the enhanced post-seismic subsidence is due to viscous flow in the lower crust balancing the gradient of gravitational potential energy generated by slip on the fault. In contrast, models involving moderate to steep faults to depths of 10 km predict uplift of the south margin and uplift-to-subsidence ratios of 1:3.1 and 1:2.2 for 45° to 60° faults, respectively, within the range of estimates from geological observations (Figs. 3C and 3D) (McNeill et al., 2005, 2007). Crustal thickness in the Eratini-Aigion area is ~33–40 km (Sachpazi, et al. 2007); we note that reducing the crustal thickness of our model from 40 km to 30 km results in uplift-to-subsidence ratios of 1:2.3 and 1:1 for models 2a and 2b respectively, providing an even better match to the geologically constrained ratios (Fig. DR6). Our models show that LANFs result in 2.2× more coseismic extension than planar 60° dipping faults for the same amount of normal slip (Fig. DR3). These findings, together with the fact that high-angle planar faults can account for the amount of total extension across the rift (Bell et al., 2011; Ford et al., 2013), lead us to conclude that high-angle normal faulting is the dominant mechanism of strain accommodation in the Corinth Rift. We support the conclusion of Lambotte et al. (2014) that if a LANF does exist in the western Corinth Rift, it is incipient.

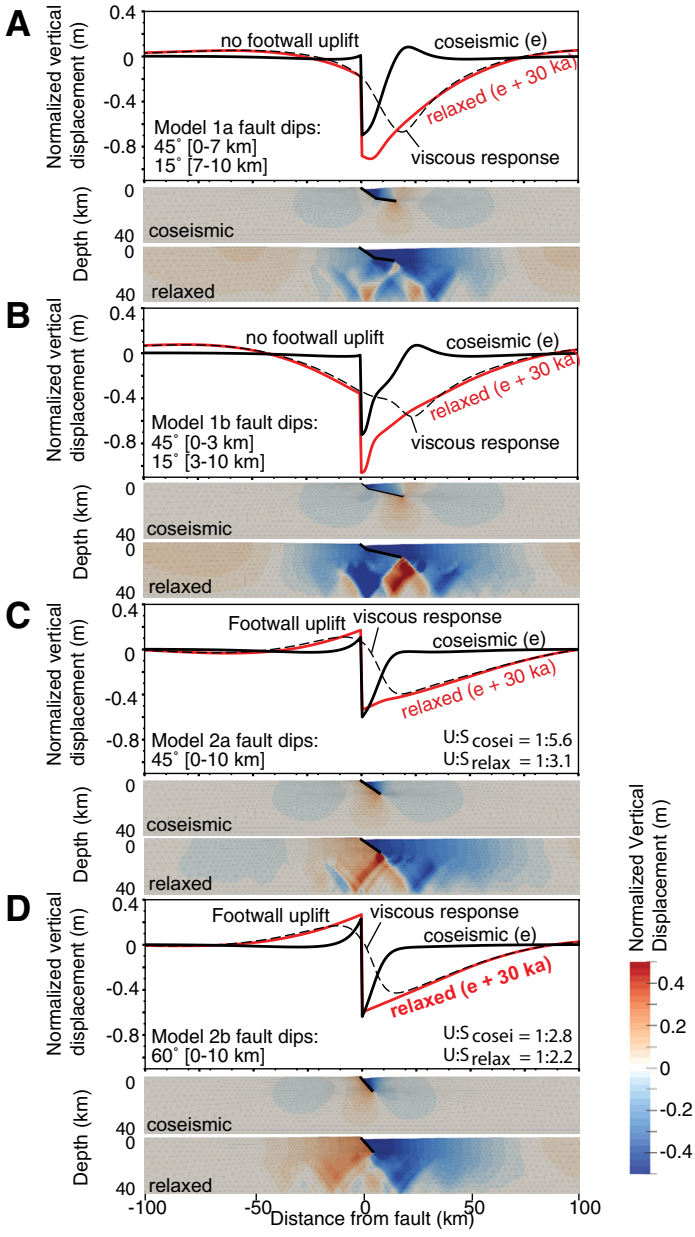

Figure 3. Effect of changing fault geometry on coseismic and long-term displacement field, per meter of slip on normal fault in 40-km-thick layered viscoelastic crust. Graph shows displacement of Earth's surface, and colored models show vertical displacements in two dimensions for coseismic slip and after 30 k.y. of post-seismic relaxation. e—coseismic vertical displacement; $U:S_{cosei}$—coseismic uplift to subsidence ratio; $U:S_{relax}$—uplift to subsidence ratio after 30 k.y. A: Model 1a: fault dipping at 45° from surface to 7 km depth, then 15° to 10 km (brittle-ductile transition). B: Model 1b: fault dipping at 45° from surface to 3 km depth, then 20° down to 10 km. C: Model 2a: planar fault dipping at 45° from surface down to 10 km. D: Model 2b: planar fault dipping at 60° from surface down to 10 km.

The elimination of the Corinth Rift as an example of a rift that deforms predominantly by low-angle normal faulting brings into question the importance of LANFs at early rift zones generally. LANFs are observed in continental rifts that (1) have undergone significant stretching and are close to breakup (e.g., Woodlark Rift, Papua New Guinea; Taylor et al. 1999), (2) exhibit significant magmatic activity or base-crustal shear stress to rotate stress tensors (e.g., Basin and Range and central Apennines), or (3) have preexisting thrust faults optimally orientated for reactivation (e.g., central Apennines). The Corinth Rift is an example of a mildly stretched rift, which is amagmatic, and normal faulting is perpendicular to the Hellenide orogeny; thus none of these conditions apply. We suggest that although LANFs can become important in the transition to breakup, high-angle faulting would be the dominant strain accommodation mechanism in areas that have undergone limited stretching, do not have significant magmatic activity, and do not have optimally orientated preexisting low-angle structures.

ACKNOWLEDGMENTS

We would like to thank Brian Taylor, Charles Williams, and Rosa Polanco-Ferrer for insightful discussions. We thank the Computational Infrastructure for Geodynamics (https://geodynamics.org), which is funded by the U.S. National Science Foundation under award NSF-0949446. R.L. Gawthorpe acknowledges the Research Council of Norway PETROMAKS 2 Syn-rift Systems Project (255229/E30). Thanks to Mary Ford, Giovanni Camanni, an anonymous reviewer, and editor Dennis Brown for constructive comments.

REFERENCES CITED

Aagaard, B.T., Knepley, M.G., and Williams, C.A., 2013, A domain decomposition approach to implementing fault slip in finite-element models of quasi-static and dynamic crustal deformation: Journal of Geophysical Research: Solid Earth, v. 118, p. 3059–3079, https://doi.org/10.1002/jgrb.50217.

Anderson, E.M., 1905, The dynamics of faulting: Transactions of the Edinburgh Geological Society, v. 8, p. 387–402.

Armijo, R., Meyer, B., King, G.C.P., Rigo, A., and Papanastassiou, D., 1996, Quaternary evolution of the Corinth Rift and its implications for the Late Cenozoic evolution of the Aegean: Geophysical Journal International, v. 126, p. 11–53, https://doi.org/10.1111/j.1365-246X.1996.tb05264.x.

Bell, R.E., McNeill, L.C., Bull, J.M., Henstock, T.J., Collier, R.E.L., and Leeder, M.R., 2009, Fault architecture, basin structure and evolution of the Gulf of Corinth Rift, central Greece: Basin Research, v. 21, p. 824–855, https://doi.org/10.1111/j.1365-2117.2009.00401.x.

Bell, R.E., McNeill, L.C., Henstock, T.J., and Bull, J.M., 2011, Comparing extension on multiple time and depth scales in the Corinth Rift, Central Greece: Geophysical Journal International, v. 186, p. 463–470, https://doi.org/10.1111/j.1365-246X.2011.05077.x.

Bernard, P., et al., 1997, The M_s = 6.2, June 15, 1995 Aigion earthquake (Greece): Evidence for low angle normal faulting in the Corinth rift: Journal of Seismology, v. 1, p. 131–150, https://doi.org/10.1023/A:1009795618839.

Collettini, C., De Paola, N., Holdsworth, R.E., and Barchi, M.R., 2006, The development and behaviour of low-angle normal faults during Cenozoic asymmetric extension in the Northern Apennines, Italy: Journal of Structural Geology, v. 28, p. 333–352, https://doi.org/10.1016/j.jsg.2005.10.003.

Elias, P., Kontoes, C., Papoutsis, I., Kotsis, I., Marinou, A., Paradissis, D., and Sakellariou, D., 2009, Permanent Scatterer InSAR analysis and validation in the Gulf of Corinth: Sensors (Basel), v. 9, https://doi.org/10.3390/s90100046.

Ford, M., Rohais, S., Williams, E.A., Bourlange, S., Jousselin, D., Backert, N., and Malartre, F., 2013, Tectono-sedimentary evolution of the western Corinth rift (Central Greece): Basin Research, v. 25, p. 3–25, https://doi.org/10.1111/j.1365-2117.2012.00550.x.

Gessner, K., Ring, U., Johnson, C., Hetzel, R., Passchier, C.W., and Güngör, T., 2001, An active bivergent rolling-hinge detachment system: Central Menderes metamorphic core complex in western Turkey: Geology, v. 29, p. 611–614, https://doi.org/10.1130/0091-7613(2001)029<0611:AABRHD>2.0.CO;2.

Ghisetti, F., and Vezzani, L., 1999, Depth and modes of Pliocene–Pleistocene crustal extension of the Apennines (Italy): Terra Nova, v. 11, p. 67–72, https://doi.org/10.1046/j.1365-3121.1999.00227.x.

Jackson, J.A., Gagnepain, J., Houseman, G., King, G.C.P., Papadimitriou, P., Soufleris, C., and Virieux, J., 1982, Seismicity, normal faulting, and the geomorphological development of the Gulf of Corinth (Greece): The Corinth earthquakes of February and March 1981: Earth and Planetary Science Letters, v. 57, p. 377–397, https://doi.org/10.1016/0012-821X(82)90158-3.

Jolivet, L., Labrousse, L., Agard, P., Lacombe, O., Bailly, V., Lecomte, E., Mouthereau, F., and Mehl, C., 2010, Rifting and shallow-dipping detachments, clues from the Corinth Rift and the Aegean: Tectonophysics, v. 483, p. 287–304, https://doi.org/10.1016/j.tecto.2009.11.001.

King, T.A., 1998, Mechanisms of isostatic compensation in areas of lithospheric extension: Examples from the Aegean [Ph.D. thesis]: Leeds, UK, University of Leeds, 355 p.

Lambotte, S., Lyon-Caen, H., Bernard, P., Deschamps, A., Patau, G., Nercessian, A., Pacchiani, F., Bourouis, S., Drilleau, M., and Adamova, P., 2014, Reassessment of the rifting process in the Western Corinth Rift from relocated seismicity: Geophysical Journal International, v. 197, p. 1822–1844, https://doi.org/10.1093/gji/ggu096.

Lecomte, E., Le Pourhiet, L., and Lacombe, O., 2012, Mechanical basis for slip along low-angle normal faults: Geophysical Research Letters, v. 39, L03307, https://doi.org/10.1029/2011GL050756.

McNeill, L.C., Collier, R.E.L., De Martini, P.M., Pantosti, D., and D'Addezio, G., 2005, Recent history of the Eastern Eliki Fault, Gulf of Corinth: Geomorphology, palaeoseismology and impact on palaeoenvironments: Geophysical Journal International, v. 161, p. 154–166, https://doi.org/10.1111/j.1365-246X.2005.02559.x.

McNeill, L.C., Cotterill, C.J., Bull, J.M., Henstock, T.J., Bell, R., and Stefatos, A., 2007, Geometry and slip rate of the Aigion fault, a young normal fault system in the western Gulf of Corinth: Geology, v. 35, p. 355–358, https://doi.org/10.1130/G23281A.1.

Nixon, C.W., et al., 2016, Rapid spatiotemporal variations in rift structure during development of the Corinth Rift, central Greece: Tectonics, v. 35, p. 1225–1248, https://doi.org/10.1002/2015TC004026.

Parsons, T., and Thompson, G.A., 1993, Does magmatism influence low-angle normal faulting?: Geology, v. 21, p. 247–250, https://doi.org/10.1130/0091-7613(1993)021<0247:DMILAN>2.3.CO;2.

Resor, P.G., 2008, Deformation associated with a continental normal fault system, western Grand Canyon, Arizona: Geological Society of America Bulletin, v. 120, p. 414–430, https://doi.org/10.1130/B26107.1.

Rigo, A., Lyon-Caen, H., Armijo, R., Deschamps, A., Hatzfeld, D., Makropoulos, K., Papadimitriou, P., and Kassaras, I., 1996, A microseismic study in the western part of the Gulf of Corinth (Greece): Implications for large-scale normal faulting mechanisms: Geophysical Journal Internatio nal, v. 126, p. 663–688, https://doi.org/10.1111/j.1365-246X.1996.tb04697.x.

Sachpazi, M., Clément, C., Laigle, M., Hirn, A., and Roussos, N., 2003, Rift structure, evolution, and earthquakes in the Gulf of Corinth, from reflection seismic images: Earth and Planetary Science Letters, v. 216, p. 243–257, https://doi.org/10.1016/S0012-821X(03)00503-X.

Sachpazi, M., Galvé, A., Laigle, M., Hirn, A., Sokos, E., Serpetsidaki, A., Marthelot, J.-M., Pi Alperin, J.M., Zelt, B., and Taylor, B., 2007, Moho topography under central Greece and its compensation by Pn time-terms for the accurate location of hypocenters: The example of the Gulf of Corinth 1995 Aigion earthquake: Tectonophysics, v. 440, p. 53–65, https://doi.org/10.1016/j.tecto.2007.01.009.

Sorel, D., 2000, A Pleistocene and still-active detachment fault and the origin of the Corinth-Patras rift, Greece: Geology, v. 28, p. 83–86, https://doi.org/10.1130/0091-7613(2000)28<83:APASDF>2.0.CO;2.

Taylor, B., Goodliffe, A.M., and Martinez, F., 1999, How continents break up: Insights from Papua New Guinea: Journal of Geophysical Research, v. 104, p. 7497–7512, https://doi.org/10.1029/1998JB900115.

Taylor, B., Weiss, J.R., Goodliffe, A.M., Sachpazi, M., Laigle, M., and Hirn, A., 2011, The structures, stratigraphy and evolution of the Gulf of Corinth rift, Greece: Geophysical Journal International, v. 185, p. 1189–1219, https://doi.org/10.1111/j.1365-246X.2011.05014.x.

Manuscript received 26 July 2017
Revised manuscript received 30 October 2017
Manuscript accepted 2 November 2017

Printed in USA